Engineering Journal issn: 0125-8281

Article

An Evaluation of the Accuracy of GNSS Receivers Integrated with MEMS-IMU Sensors for Optimal Angle Determination in Tilted Observation Scenarios Using the NRTK GNSS Technique in Thailand

Teetat Charoenkalunyuta[1,a], **Chalermchon Satirapod**[1,b,*], **Koltouch Anantakarn**[1,c], **and Thayathip Thongtan**[2,d]

1 Mapping and Positioning from Space (MAPS) Research Center, Department of Survey Engineering, Faculty of Engineering, Chulalongkorn University, Bangkok, Thailand

2 National Institute of Metrology (Thailand), Pathumthani, Thailand

E-mail: [a]teetat.c@chula.ac.th, [b,*]Chalermchon.s@chula.ac.th (Corresponding author), [c]kn.koltouch@gmail.com, [d]thayathip@nimt.or.th

Abstract. This paper evaluates the performance and accuracy of GNSS receivers integrated with MEMS-IMU sensors for optimal angle determination in tilted observation scenarios within obstructed environments. Utilizing the Network-based RTK (NRTK) GNSS technique, two GNSS receiver brands, Tersus Oscar (OS) and e-Survey E600, were tested at various tilt angles, ranging from 0° to 60°, at specific locations on the rooftop of the Engineering Building at Chulalongkorn University, Bangkok, Thailand. These test points included open areas and obstructed positions, such as corners and doors, where satellite visibility is reduced. The study assesses the Root Mean Square Error (RMSE) in both horizontal and vertical positions, as well as the Position Dilution of Precision (PDOP). Results indicate that horizontal accuracy decreases with increased tilt angles in obstructed environments, with the 'Door' point showing the highest errors due to significant obstructions. Conversely, 'Corner right' consistently demonstrates superior accuracy across all conditions. The integration of tilt-compensation technology is shown to improve positioning precision, especially in challenging environments where physical obstructions affect satellite signal reception. This research provides valuable insights for improving the accuracy of GNSS-based cadastral surveys and other high-precision applications in obstructed environments.

Keywords: MEMS-IMU sensors, network-based RTK GNSS, title observation.

ENGINEERING JOURNAL Volume 28 Issue 11
Received 19 September 2024
Accepted 6 November 2024
Published 30 November 2024
Online at https://engj.org/
DOI:10.4186/ej.2024.28.11.99

DOI:10.4186/ej.2024.28.11.99

1. Introduction

The GNSS (Global Navigation Satellite System) serves as an electronic tool for computing and presenting positions using satellite signals. Advancements in GNSS receivers have led to the emergence of the Network-based Real-Time Kinematic (NRTK) GNSS technique, which is widely used in cadastral surveys. This technique involves several sequential steps: Continuously Operating Reference Stations (CORS) initially receive satellite signals and continuously record observation data, which is then transmitted to control centers. Following this, rovers are stationed at desired coordinate points, connecting to the internet to send approximate coordinate data to control centers. Subsequently, control center processing systems generate virtual reference station positions (VRS) near the rover device. Finally, positioning calculations are performed from the VRS, resembling the single RTK technique but with shorter baseline distances and improved accuracy [1-7].

Survey marks are fundamental to cadastral surveying, providing the physical reference points necessary for accurate property boundary determination. GNSS technology, combined with Network-based RTK, enhances the accuracy and efficiency of establishing and maintaining these marks. Despite challenges, careful placement, documentation, and regular verification ensure the reliability of survey marks, supporting legal, developmental, and construction activities. However, when survey marks are located at the corner of a building, the structure may block satellite signals to the GNSS receiver, potentially affecting the accuracy of the measurements (see Fig. 1).

Fig. 1. The GNSS receiver is located at the corner of a building on the survey marks.

To address challenges in cadastral survey, numerous GNSS receiver equipment manufacturers have integrated Inertial Measurement Units (IMU) sensors into their GNSS receivers by MEMS (Micro-Electro-Mechanical Systems) technology [8-14]. This integration helps compensate for device tilting, ensuring precise positioning, especially in demanding environments. While GNSS receivers excel in receiving satellite signals for accurate positioning, they often encounter difficulties in adverse environmental conditions. Obstacles or interference can hinder their ability to provide precise or efficient positioning. Therefore, the effectiveness of these GNSS receivers utilizing the NRTK GNSS technique was tested to evaluate various tilt compensation sensor angles in fieldwork.

2. Literature Review

These sections consist of three sub-sections described as follows:

2.1. Network-Based RTK GNSS in Thailand

Network-based Real-Time Kinematic (RTK) GNSS services in Thailand are provided by key entities such as the Department of Lands (DOL) and the National CORS Data Center (NCDC), which collectively enhance the accuracy and reliability of GNSS measurements through a network of CORS. The Department of Lands operates an extensive CORS network designed to support high-precision applications in surveying, mapping, and land registration. This network delivers real-time correction data that enables users to achieve centimeter-level positional accuracy, crucial for cadastral surveys and other geospatial tasks by using Virtual Reference Station (VRS) technique [7, 15]. The CORS infrastructure provided by the Department of Lands is pivotal in ensuring that land-related data is accurate and reliable, facilitating efficient land management and legal land documentation processes.

Similarly, the National CORS Data Center offers a comprehensive suite of GNSS data services that cater to a wide array of applications, from geodetic surveys to agriculture and navigation. The center's CORS network provides real-time correction signals essential for RTK GNSS operations, significantly improving positional accuracy by using VRS technique as well [16-18]. This high level of precision supports various industries, including construction, where precise positioning is critical for project accuracy and efficiency. Additionally, the agricultural sector benefits from these services through enhanced precision farming techniques that optimize resource use and increase crop yields. The National CORS Data Center’s services ensure that users across different sectors can rely on accurate and timely GNSS data for their operations.

The VRS technique in NRTK GNSS systems significantly enhances positional accuracy by leveraging a network of CORS. This advanced method starts with the continuous collection of GNSS data from multiple CORS, which is then sent to a central server for processing. The central server models atmospheric and satellite corrections over the entire area covered by the network. When a user initiates a request, the system uses the initial GNSS data to approximate the user's position and subsequently generates a virtual reference station (VRS) near the user's actual location. This virtual station acts as if it were a physical reference point, providing highly localized correction data. The correction information from the VRS is then transmitted to the user's RTK receiver, which applies these corrections to achieve centimeter-level positional accuracy. This approach not only extends the effective coverage area of the CORS network, making high-precision GNSS applications possible even in regions with sparse physical reference stations, but also enhances efficiency by eliminating the need for users to set up their own base stations[1-7]. The VRS technique is particularly beneficial for applications requiring high accuracy, such as surveying, construction, agriculture, and other geospatial tasks, as it ensures robust, reliable, and precise geospatial data, thereby improving productivity and accuracy across various professional and industrial domains. Moreover, [7] assesses the performance of Thai-NRTK GNSS in VRS mode for cadastral survey in Thailand. Results show that the horizontal Root Mean Square Error (RMSE) below 4 cm for all the network, meeting accuracy requirements of The Department of Lands Regulation of the practical RTK GNSS Network for the Cadastral Survey B. E. 2562 [7, 19].

Together, these networks from the Department of Lands and the National CORS Data Center ensure that Thailand's geospatial infrastructure is robust, reliable, and capable of supporting the growing demand for high-accuracy positioning data. Through continuous maintenance and technological advancements, these services provide essential support for the nation's geospatial needs, driving improvements in efficiency and accuracy in various professional and industrial applications. This collaboration between different service providers illustrates a comprehensive approach to leveraging GNSS technology for national development and precision-based applications in Thailand.

2.2. GNSS Receivers Integrated with MEMS-IMU Sensors

The development of GNSS receivers integrated with IMU sensors has significantly advanced over the past two decades. Initially, tilt compensation in GNSS rovers utilized magnetic compass orientation, which required complex calibration and was prone to magnetic disturbances, limiting its effectiveness and user acceptance [14]. The integration of GNSS with inertial measurement units (IMUs) marked a significant leap forward, providing enhanced navigation and positioning accuracy. This integration, commonly known as the GNSS inertial navigation system (INS), employs a three-axis accelerometer and gyroscope within the IMU to measure tilt and correct positional errors [14].

With advancements in MEMS technology, the development of integrated GNSS/IMU systems began. MEMS-IMU sensors, which include accelerometers and gyroscopes, enabled more reliable and accurate tilt measurements and orientation corrections. These developments marked a significant leap forward, allowing for the creation of GNSS inertial navigation systems (INS) that could provide continuous and accurate positioning data even in environments where GNSS signals were weak or obstructed [11].

The basic data processing schematic of an IMU-based tilted RTK receiver involves several critical steps to ensure high-accuracy positioning, even when the receiver is tilted. Initially, raw data is collected from both GNSS satellites and IMU sensors, where the GNSS data provides the primary positional information, and the IMU data offers detailed insights into the receiver's orientation and motion. This raw data undergoes pre-processing to correct atmospheric errors, multipath effects, and sensor noise, ensuring that the data is as accurate and reliable as possible. Following pre-processing, an initial alignment step is performed to determine the receiver's tilt and orientation relative to the GNSS reference frame. This alignment is crucial for integrating the GNSS and IMU data correctly. The core of the data processing schematic is the data fusion step, typically performed using a Kalman filter. This advanced algorithm integrates the high-frequency IMU data with the lower-frequency but more accurate GNSS data, continuously updating the receiver's position and orientation estimates. Through this fusion process, the system can perform real-time tilt compensation, adjusting the GNSS-derived position based on the IMU data to reflect the receiver's actual location accurately. Finally, the tilt-compensated position is calculated and output, providing precise and reliable geolocation data suitable for applications such as surveying, mapping, and navigation. This integrated approach allows the system to maintain high positional accuracy, even in challenging environments where the receiver might not be perfectly level [11, 14].

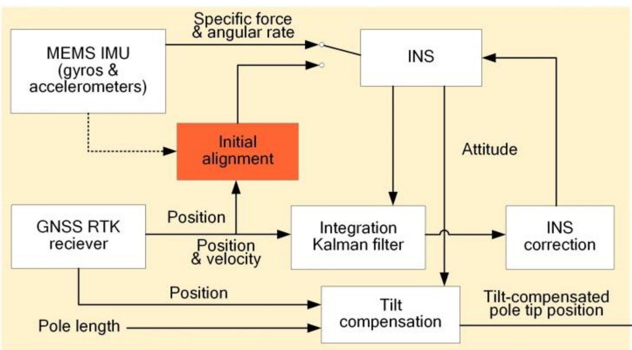

Fig. 2.“Basic data processing schematic of the IMU-based tilted RTK receiver” [10].

Several studies address the challenges and advancements in GNSS/IMU integration for accurate positioning in urban environments and tilted observation scenarios. Carrier-phase-based high-accuracy positioning remains difficult in urban settings even with expensive dual-frequency receivers. However, tightly integrating single-frequency multi-GNSS RTK with low-cost MEMS-IMU, along with outlier-resistant ambiguity resolution (AR) and Kalman filtering, significantly enhances performance, showing improved positioning accuracy, reliability, higher fixing rates, and reduced errors compared to single- and dual-frequency RTK [8]. Enhancing tightly coupled GNSS/IMU/odometry integration by incorporating multi-constellation, multi-frequency GNSS observations and odometry measurements has shown improvements, with successful calibration of differential code biases (DCBs) and the addition of Galileo satellites improving measurement availability and positioning performance [9]. For tilted RTK surveys, a proposed method determines the initial INS heading from the angle between INS and RTK-indicated trajectories, showing that this method can determine initial heading to 1.15° within 2-3 seconds, significantly improving the efficiency and accuracy of tilted RTK receivers [10]. A GNSS/INS tight integration system using multiple receivers, specifically three self-developed DSPC-FPGA receivers, showed improved navigation accuracy compared to single-receiver systems, with a measurement difference method introduced to reduce the state vector's dimension and computational load [11]. Evaluations of GNSS receivers with tilt sensors, including magnetometer, MEMS, and IMU, for accurate positioning of parcel boundaries, showed that IMU sensors provided better horizontal accuracy, achieving better than 4 cm accuracy at up to 15° tilt in open-sky conditions, although none accurately compensated for tilt in complex, multipath environments [13]. An experiment evaluating the accuracy and reliability of seven GNSS/IMU receivers underscored the importance of tilt compensation, particularly for cadastral surveys, although it is viable only when the required accuracy is within 5 cm [14].

2.3. PDOP

The Position Dilution of Precision (PDOP) quantifies the effect of satellite geometry on the precision of a GNSS position fix. It combines horizontal (HDOP) and vertical (VDOP) dilution of precision, representing the three-dimensional positioning accuracy. Lower PDOP values (close to 1) indicate a well-distributed satellite constellation, resulting in more accurate and reliable positioning. Higher PDOP values suggest poor satellite geometry, leading to less accurate positioning. [20, 21]

3. Methodology

The methodology for this study is designed to evaluate the horizontal accuracy of GNSS + MEMS-IMU receivers under different environmental conditions: open area and obstructed area. The approach involves both static and tilted observations to comprehensively assess the performance of the GNSS + MEMS-IMU receivers. The research is conducted at the rooftop of Engineering 4 Building, Chulalongkorn University, Bangkok, Thailand as illustrated in Fig. 3. Point 'Top' is situated in open areas, whereas points 'Door'' and 'Corner' are in obstructed area conditions.

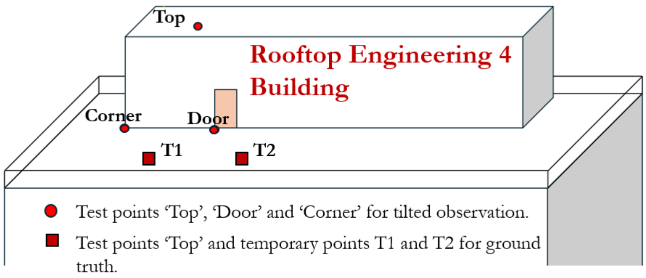

Fig. 3. The environmental conditions: open area and obstructed area.

The study is divided into three key sections: static observation, tilted observation and evaluation of horizontal accuracy (see Fig. 4) as explained follow:

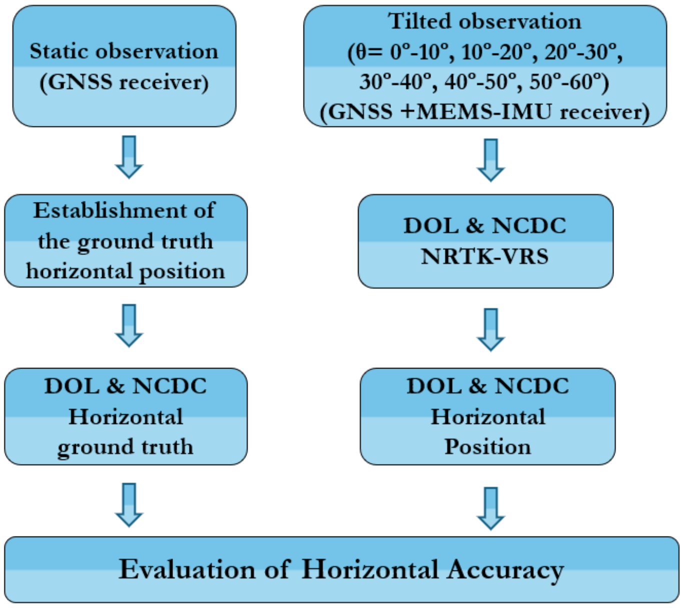

Fig. 4. Concept of computation algorithm.

3.1. Static Observation

On August 11, 2023, a two-hour static observation was conducted at 30-second intervals at the test point 'Top' and two temporary points, labeled T1 and T2, situated in an open area. The Tersus Oscar GNSS Receiver was employed to establish accurate horizontal ground truth positions. The collected static data was subsequently processed using Tersus Geomatics Office (TGO) version 1.1, a commercial software, applying the post-processing static method. This process utilized RINEX data from three Continuously Operating Reference Stations (CORSs) supplied by the Department of Lands (DOL) and the National Control Data Center (NCDC) as reference

DOI:10.4186/ej.2024.28.11.99

points. The resulting accuracy of these ground truth points is approximately 2 centimeters (see Fig. 5).

Fig. 5. A two-hour static observation was collected at 30-second intervals at test point A, and temporary points T1 and T2.

The ground truth for test points 'Door' and 'Corner' was established in an obstructed area by measuring distances from reference points T1 and T2 using a steel tape. These measurements were used in the Two Point Intersection method to determine the positions accurately. The Nuwa function on the Tersus TC50 controller was employed for this intersection process (as shown in Fig. 6). Consequently, the ground truth positions for 'Door' and 'Corner' were derived from the known positions of temporary reference points T1 and T2, ensuring reliable accuracy despite the obstructions.

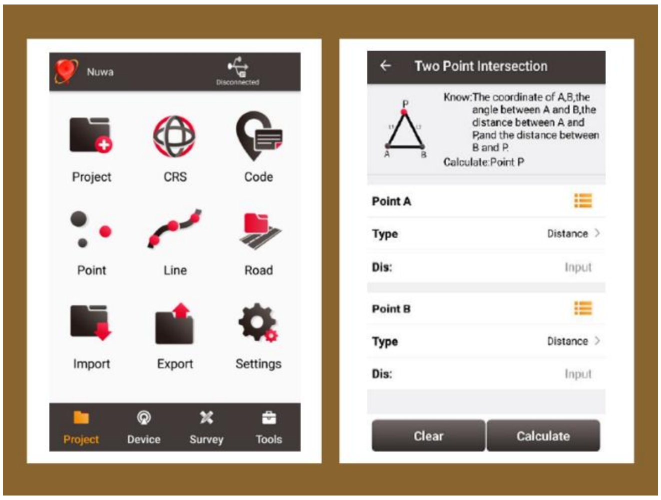

Fig. 6. Two points intersection by distance function.

3.2. Tilted Observations by GNSS + MEMS-IMU Receiver

Tilted observations, displaying the angle from the vertical on the controller, were conducted at all test points 'Top' and 'Door', while the 'Corner_left' and 'Corner_right' were conducted at 'Corner' point (see Fig. 7 Below). These observations were performed at various group angles (θ) of 0º-10º, 10º-20º, 20º-30º, 30º-40º, 40º-50º, and 50º-60º from the vertical (see Fig. 7 top), using two different GNSS+MEMS-IMU receivers: the Tersus Oscar GNSS and the e-survey E600 GNSS receivers (denoted as OS and E600 respectively). To simulate real-world conditions and assess the impact on horizontal accuracy, both DOL and NCDC NRTK-VRS service providers were used. Each tilted observation at each test point and group angle for each receiver was recorded at 60-second intervals (see Figure 8.). The results of this section present the DOL and NCDC horizontal positions separately.

3.3. Evaluation of Horizontal Accuracy

Horizontal accuracy was evaluated by comparing the results from the DOL and NCDC ground truth data (as described in section 4.1) with the DOL and NCDC horizontal positions obtained from NRTK-VRS (as described in section 4.2). The statistical measure used to assess horizontal and vertical accuracy in this study is the Horizontal and Vertical RMSE (Root Mean Square Error), as specified in Eq. (1) and (2), respectively. [16, 22].

$$RMSE_{Hor} = \sqrt{\frac{\Sigma((N_{GT} - Ni_{OBS})^2 + (E_{GT} - Ei_{OBS})^2)}{n}} \tag{1}$$

where

$RMSE_{Hor}$ is the RMSE of horizontal position (meter),
N_{GT} is the ground truth of the north-south position (meter),
N_{OBS} is the north-south position in tilted observation (meter),
E_{GT} is the ground truth of the east-west position (meter),
E_{OBS} is the east-west position in tilted observation (meter),
i is the measurement number in a 1-second epoch recorded at 60-second intervals,
n is the number of test points.

$$RMSE_{Ver} = \sqrt{\frac{\Sigma((V_{GT} - Vi_{OBS})^2)}{n}} \tag{2}$$

where

$RMSE_{Ver}$ is the RMSE of vertical position (meter),
V_{GT} is the ground truth of the vertical position (meter),
V_{OBS} is the vertical position in tilted observation (meter),
i is the measurement number in a 1-second epoch recorded at 60-second intervals,
n is the number of test points.

DOI:10.4186/ej.2024.28.11.99

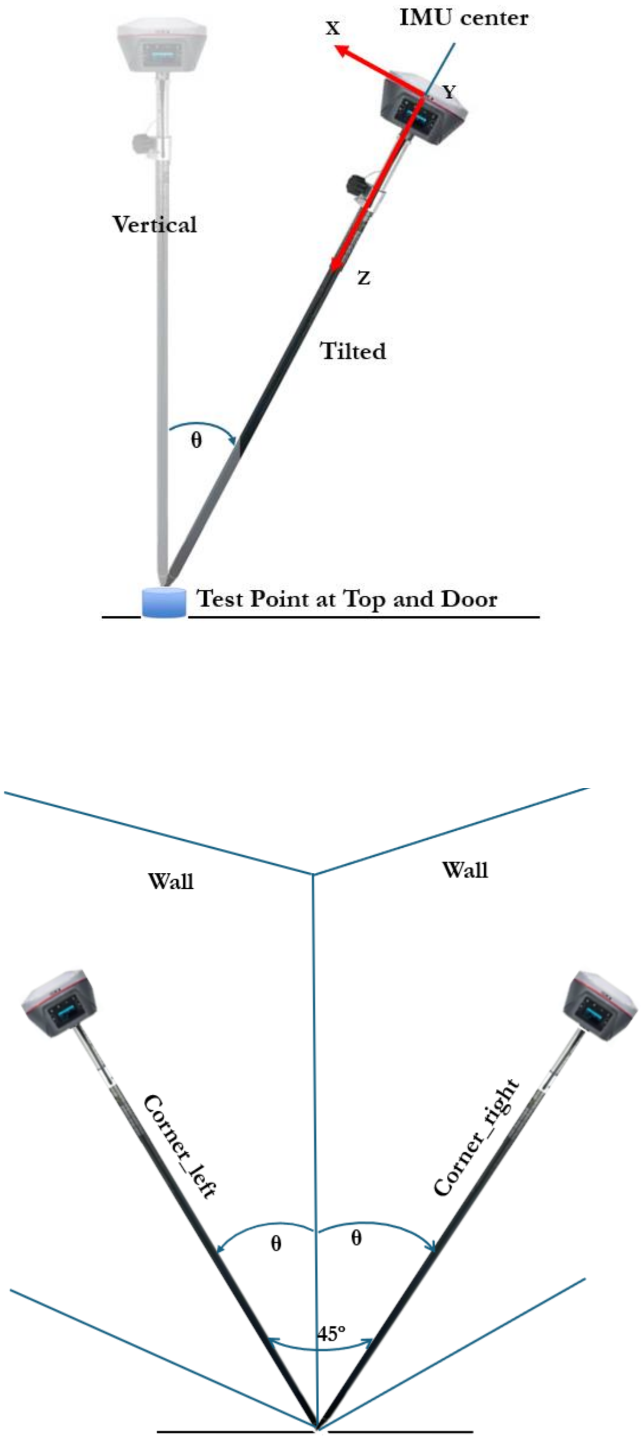

Fig. 7. Tilted observations at various group angles (θ) of 0°-10°, 10°-20°, 20°-30°, 30°-40°, 40°-50°, and 50°-60° from the vertical at points 'Top' and 'Door' (top photo) and at point 'Corner_left' and 'Corner_right' (below photo).

Fig. 8. Tilted observations were conducted at various group angles (θ) in test points 'Top' (top left photo), 'Door' (top right photo), 'Corner_left' (below left photo) and 'Corner_right' (below right photo).

4. Results and Discussion

This section can be considered to two sub-sections as follows:

4.1. Open area

The results of open area condition ('Top' point) is shown in Table 1 and illuminated in Figs. 9-11.

Figure 9 shows the relationship between RMSE horizontal and tilted angle, separated by different providers and brands. RMSE horizontal values for DOL – OS exhibit slight fluctuations across different tilt angles, with noticeable increases at higher angles. Other providers and brands display similar trends with variations in RMSE horizontal values, indicating that horizontal positioning accuracy is affected by tilt angle. Figure 10 depicts RMSE vertical in relation to tilted Angle, where RMSE Vertical values for DOL - OS fluctuate more significantly with changes in tilt angle, suggesting that vertical positioning accuracy is more sensitive to tilt. Other providers and brands show variations in patterns, with some exhibiting stable trends and others peaking at certain tilt angles. On the other hand, the PDOP remains relatively stable across tilt angles, indicating consistent satellite geometry (see Fig. 11 for details).

Table 1. Results of 'Top' point.

Provider	Brand	Tilted Angle (°)	RMSE Hor (m)	RMSE Ver (m)	PDOP	n*
DOL	OS	0-10	0.024	0.132	1.1	23
DOL	OS	11-20	0.024	0.132	1.1	55
DOL	OS	21-30	0.023	0.127	1.1	66
DOL	OS	31-40	0.027	0.129	1.1	57
DOL	OS	41-50	0.034	0.126	1.1	86
DOL	OS	51-60	0.039	0.125	1.1	77
DOL	E600	0-10	0.016	0.197	0.7	38
DOL	E600	11-20	0.025	0.195	0.6	51
DOL	E600	21-30	0.020	0.200	0.6	78
DOL	E600	31-40	0.023	0.203	0.6	75
DOL	E600	41-50	0.032	0.205	0.6	63
DOL	E600	51-60	0.031	0.207	0.7	49
NCDC	OS	0-10	0.055	0.034	1.1	21
NCDC	OS	11-20	0.050	0.013	1.1	33
NCDC	OS	21-30	0.050	0.017	1.1	36
NCDC	OS	31-40	0.053	0.021	1.1	38
NCDC	OS	41-50	0.053	0.023	1.1	37
NCDC	OS	51-60	0.054	0.014	1.1	40
NCDC	E600	0-10	0.036	0.103	0.6	54
NCDC	E600	11-20	0.030	0.108	0.6	43
NCDC	E600	21-30	0.038	0.109	0.6	64
NCDC	E600	31-40	0.035	0.110	0.7	49
NCDC	E600	41-50	0.041	0.113	0.7	53
NCDC	E600	51-60	0.042	0.114	0.7	44

n* is the number of test points.

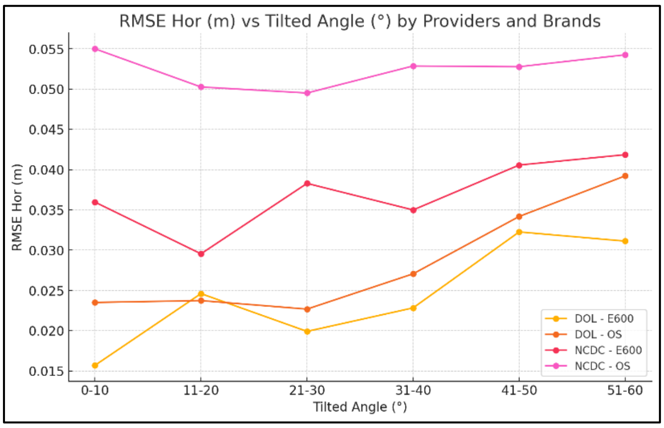

Fig. 9. Illuminated RMSE Horizontal (m) vs. Tilted angle (°) for the Open area separated by different providers and brands.

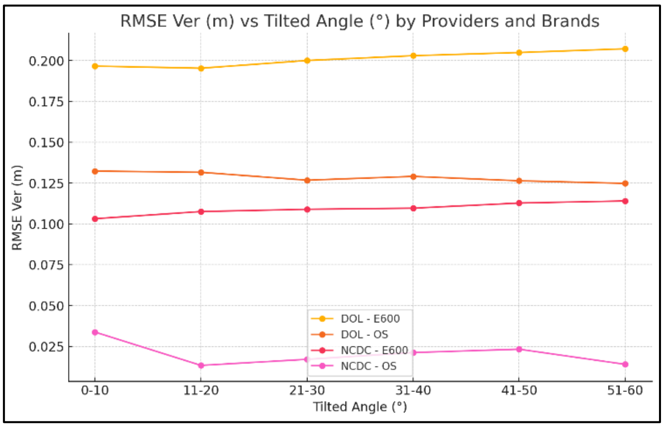

Fig. 10. Illuminated RMSE Vertical (m) vs. Tilted angle (°) for the Open area separated by different providers and brands.

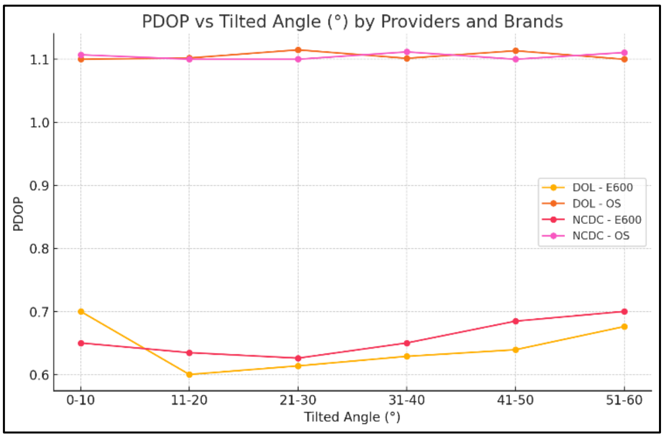

Fig. 11. Illuminated PDOP vs. Tilted angle (°) for the Open area separated by different providers and brands.

4.2. Obstructed Area

The results of obstructed area condition are shown in Tables 2-4 and illuminated in Figs. 12-14 as well.

In the obstructed area, as illustrated in Figs. 12 to 14 for the "Door," "Corner left," and "Corner right" positions across different tilt angles, separated by providers and brands, clear trends emerge in RMSE Horizontal, RMSE Vertical, and PDOP as tilt angles increase. RMSE Horizontal generally decreases or stabilizes for both 'Corner' positions, with 'Corner_right' showing better horizontal accuracy across all providers. However, the 'Door' point demonstrates increasing horizontal errors, particularly in the DOL - E600 and NCDC - OS brands, indicating that obstruction has a more significant impact at this location. RMSE Vertical is relatively low for the 'Corner' positions but is consistently higher for the 'Door' point, especially for the NCDC - OS provider, where vertical errors exceed 1 meter. PDOP remains stable across all positions, but the 'Door' point exhibits higher PDOP values compared to the 'Corner' positions, suggesting poorer satellite geometry. Overall, 'Corner_right' performs best in both horizontal and vertical accuracy, while the 'Door' point shows the greatest

DOI:10.4186/ej.2024.28.11.99

degradation in accuracy due to the obstructed environment.

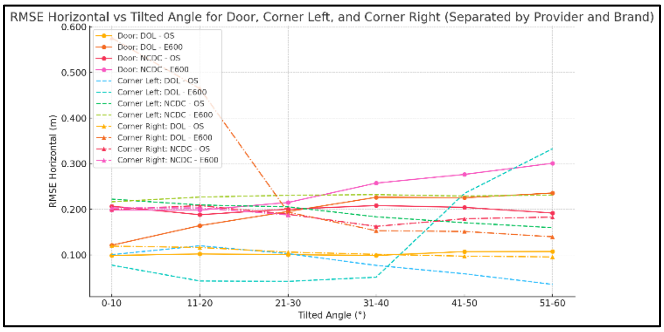

Fig. 12. Illuminated RMSE Horizontal (m) vs. Tilted angle (°) for the Obstructed area separated by different providers and brands.

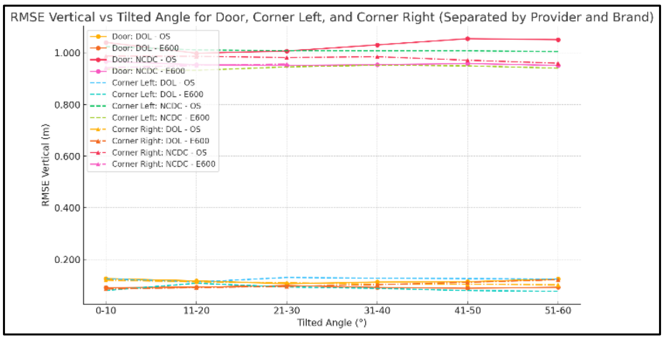

Fig. 13. Illuminated RMSE Vertical (m) vs. Tilted angle (°) for the Obstructed area separated by different providers and brands.

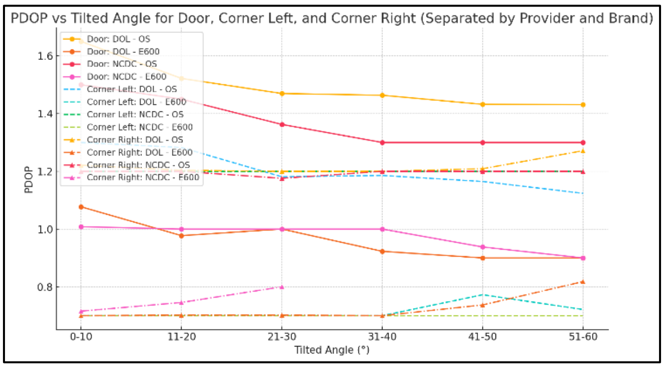

Fig. 14. Illuminated PDOP vs. Tilted angle (°) for the Obstructed area separated by different providers and brands.

Table 2. Results of 'Door' point.

Provider	Brand	Tilted Angle (°)	RMSE Hor (m)	RMSE Ver (m)	PDOP	n*
DOL	OS	0-10	0.099	0.126	1.7	24
DOL	OS	11-20	0.102	0.117	1.5	32
DOL	OS	21-30	0.101	0.106	1.5	33
DOL	OS	31-40	0.099	0.112	1.5	22
DOL	OS	41-50	0.107	0.114	1.4	28
DOL	OS	51-60	0.107	0.124	1.4	16
DOL	E600	0-10	0.121	0.091	1.1	35
DOL	E600	11-20	0.164	0.093	1.0	44
DOL	E600	21-30	0.195	0.099	1.0	48
DOL	E600	31-40	0.226	0.092	0.9	48
DOL	E600	41-50	0.225	0.089	0.9	50
DOL	E600	51-60	0.236	0.092	0.9	34
NCDC	OS	0-10	0.207	1.040	1.5	16
NCDC	OS	11-20	0.188	0.998	1.5	20
NCDC	OS	21-30	0.200	1.007	1.4	16
NCDC	OS	31-40	0.208	1.031	1.3	30
NCDC	OS	41-50	0.204	1.055	1.3	24
NCDC	OS	51-60	0.192	1.051	1.3	30
NCDC	E600	0-10	0.198	0.967	1.0	24
NCDC	E600	11-20	0.198	0.954	1.0	48
NCDC	E600	21-30	0.215	0.951	1.0	41
NCDC	E600	31-40	0.257	0.954	1.0	31
NCDC	E600	41-50	0.277	0.959	0.9	29
NCDC	E600	51-60	0.301	0.951	0.9	33

n* is the number of test points.

Table 3. Results of 'Corner_left' point.

Provider	Brand	Tilted Angle (°)	RMSE Hor (m)	RMSE Ver (m)	PDOP	n*
DOL	OS	0-10	0.100	0.125	1.3	12
DOL	OS	11-20	0.120	0.112	1.3	23
DOL	OS	21-30	0.103	0.130	1.2	37
DOL	OS	31-40	0.077	0.127	1.2	28
DOL	OS	41-50	0.059	0.126	1.2	37
DOL	OS	51-60	0.036	0.124	1.1	21
DOL	E600	0-10	0.078	0.080	0.7	28
DOL	E600	11-20	0.043	0.108	0.7	41
DOL	E600	21-30	0.042	0.093	0.7	29
DOL	E600	31-40	0.051	0.088	0.7	37
DOL	E600	41-50	0.235	0.079	0.8	40
DOL	E600	51-60	0.333	0.077	0.7	47
NCDC	OS	0-10	0.222	1.024	1.2	9
NCDC	OS	11-20	0.209	1.011	1.2	27
NCDC	OS	21-30	0.205	1.008	1.2	41
NCDC	OS	31-40	0.184	1.008	1.2	20
NCDC	OS	41-50	0.171	1.008	1.2	33
NCDC	OS	51-60	0.160	1.005	1.2	32
NCDC	E600	0-10	0.217	0.936	0.7	18
NCDC	E600	11-20	0.227	0.932	0.7	27
NCDC	E600	21-30	0.231	0.946	0.7	32
NCDC	E600	31-40	0.232	0.952	0.7	29
NCDC	E600	41-50	0.229	0.949	0.7	35
NCDC	E600	51-60	0.231	0.941	0.7	45

n* is the number of test points.

Table 4. Results of 'Corner_right' point.

Provider	Brand	Tilted Angle (°)	RMSE Hor (m)	RMSE Ver (m)	PDOP	n*
DOL	OS	0-10	0.119	0.120	1.2	47
DOL	OS	11-20	0.116	0.113	1.2	27
DOL	OS	21-30	0.106	0.110	1.2	31
DOL	OS	31-40	0.101	0.104	1.2	27
DOL	OS	41-50	0.097	0.104	1.2	33
DOL	OS	51-60	0.096	0.102	1.3	21
DOL	E600	0-10	0.576	0.085	0.7	22
DOL	E600	11-20	0.465	0.091	0.7	48
DOL	E600	21-30	0.194	0.096	0.7	53
DOL	E600	31-40	0.153	0.102	0.7	44
DOL	E600	41-50	0.151	0.111	0.7	35
DOL	E600	51-60	0.140	0.121	0.8	61
NCDC	OS	0-10	0.200	0.988	1.2	12
NCDC	OS	11-20	0.208	0.987	1.2	26
NCDC	OS	21-30	0.189	0.982	1.2	29
NCDC	OS	31-40	0.163	0.985	1.2	31
NCDC	OS	41-50	0.179	0.971	1.2	23
NCDC	OS	51-60	0.183	0.960	1.2	26
NCDC	E600	0-10	0.203	0.942	0.7	32
NCDC	E600	11-20	0.203	0.951	0.7	35
NCDC	E600	21-30	0.188	0.957	0.8	5

n* is the number of test points.

5. Conclusions and Discussion

The conclusions and discussion of this paper highlight the performance and accuracy of GNSS receivers integrated with MEMS-IMU sensors in determining optimal tilt angles in obstructed environments using the NRTK GNSS technique. The study demonstrates that in open environments, GNSS receivers exhibit minimal error, with RMSE Horizontal and Vertical remaining relatively low even at higher tilt angles. However, in obstructed environments, such as at the 'Door' and 'Corner' positions, significant variation in positioning accuracy is observed. The 'Door' position consistently shows higher errors due to signal obstructions, especially at greater tilt angles, where both horizontal and vertical errors increase, particularly for the NCDC-OS and DOL-E600 receivers. The 'Corner_right' position consistently outperforms the other points, showing better accuracy with stable RMSE values across providers, even in obstructed conditions. The study emphasizes that incorporating tilt-compensation technology significantly improves the accuracy of GNSS positioning, particularly in complex environments where signal obstruction is common. These findings are crucial for applications such as cadastral surveying, where maintaining accuracy is paramount despite environmental challenges. Additionally, the study notes that RMSE Vertical errors were elevated during the testing period (August 2023), potentially due to high ionospheric scintillation commonly experienced in low-latitude regions like Thailand, which may have affected NRTK performance. The accuracy variations observed may also relate to CORS station spacing at the test site, with differing station densities likely contributing to the positional accuracy results.

6. Future Studies

Future studies should consider the influence of satellite constellation geometry on positioning accuracy, particularly in varying latitudinal regions. In equatorial areas, such as Thailand, satellite distribution across the horizon is generally more uniform, which can contribute to reduced positional errors. In contrast, higher latitudes, such as those in Australia, often experience limited satellite coverage toward the southern horizon. This disparity may significantly affect measurements taken near building corners oriented southward, especially when the receiver is tilted at high angles. Investigating these geographic and geometric variations in satellite constellation distribution and their impact on GNSS measurements under different tilt conditions would provide valuable insights for enhancing positioning accuracy across diverse environments.

References

[1] H. Landau, U. Vollath, and X. Chen, "Virtual reference station systems," *Journal of Global Positioning Systems*, vol. 1, no. 2, pp. 137-143, 2002.

[2] G. Retscher, "Accuracy performance of virtual reference station (VRS) networks," *Journal of Global Positioning Systems*, vol. 1, no. 1, pp. 40-47, 2002.

[3] J. Santala and S. Tötterström, "On testing RTK-network virtual concept, in *FIG XXII International Congress*, Washington, DC, USA, April 19-26, 2002. 2002.

[4] L. Wanninger, "Virtual reference stations for centimeter-level kinematic positioning," in *Proceedings of the 15th International Technical Meeting of the Satellite Division of The Institute of Navigation (ION GPS 2002)*, 2002.

[5] K. M. A. Mageed, "Accuracy evaluation between GPS virtual reference station (VRS) and GPS real time kinematic (RTK) techniques," *World Applied Sciences Journal*, vol. 24, no. 9, pp. 1154-1162, 2013.

[6] M. El-Tokhey, et al., "Time influence on observational accuracy in Egyptian virtual reference stations network "VRS"," *World Applied Sciences Journal*, vol. 32, no. 1, pp. 12-17, 2014.

[7] T. Charoenkalunyuta, et al., "Performance of network-based RTK GNSS for the cadastral survey in Thailand, *International Journal of Geoinformatics*, vol. 15, no. 3, 2019.

[8] T. Li, et al., "High-accuracy positioning in urban environments using single-frequency multi-GNSS RTK/MEMS-IMU integration," *Remote Sensing*, vol. 10, no. 2, p. 205, 2018.

DOI:10.4186/ej.2024.28.11.99

[9] B. Reuper, M. Becker, and S. Leinen, “Benefits of multi-constellation/multi-frequency GNSS in a tightly coupled GNSS/IMU/Odometry integration algorithm,” *Sensors*, vol. 18, no. 9, p. 3052, 2018.
[10] Q. Chen, et al., “Rapid and accurate initial alignment of the low-cost MEMS IMU chip dedicated for tilted RTK receiver,” *GPS Solutions*, vol. 24, pp. 1-13, 2020.
[11] Z. Zhu, C. Jiang, and Y. Bo, “Performance enhancement of GNSS/MEMS-IMU tightly integration navigation system using multiple receivers,” *IEEE Access*, vol. 8, pp. 52941-52949, 2020.
[12] H. Lin, “High-precision RTK positioning with tilt compensation: Data fusion algorithm,” in *Proceedings of the 34th International Technical Meeting of the Satellite Division of The Institute of Navigation (ION GNSS+ 2021)*, 2021.
[13] P. Dumrongchai, J. Patsadutarn, and C. Satirapod, “Performance tests of geodetic receivers with tilt sensors in obstructed environments using the NRTK GNSS technique,” *Journal of Applied Geodesy*, vol. 17, no. 1, pp. 39-52, 2023.
[14] J. Gučević, S. Delčev, and O. Vasović Šimšić, “Practical limitations of using the tilt compensation function of the GNSS/IMU receiver,” *Remote Sensing*, vol. 16, no. 8, p. 1327, 2024.
[15] T. Charoenkalunyuta and C. Satirapod, “Effect of Thai ionospheric maps (THIM) model on the performance of network based RTK GPS in Thailand,” *Survey Review*, vol. 46, no. 334, 2014.
[16] T. Charoenkalunyuta, et al., “Geometric and statistical assessments on horizontal positioning accuracy in relation with GNSS CORS triangulations of NRTK positioning services in Thailand,” *International Journal of Geoinformatics*, vol. 19, no. 2, 2023.
[17] P. Dumrongchai, et al., “Performance assessment of continuously operating reference stations using the deemed rover analysis approach with NRTK GNSS technique in Thailand,” *Survey Review*, pp. 1-10, 2023.
[18] T. Charoenkalunyuta, et al., “GNSS rover receivers’ horizontal positioning accuracy assessments based on NRTK-VRS surveying,” *Survey Review*, vol. 56, no. 395, pp. 191-199, 2024.
[19] Thailand, Ministry of Interior, Department of Lands, *The Department of Lands Regulation of the Practical RTK GNSS Network for the Cadastral Survey B.E. 2562*. (in Thai) Thailand: Ministry of Interior, 2019.
[20] A. H. Phillips, “Geometrical determination of PDOP,” *Navigation*, vol. 31, no. 4, pp. 329-337, 1984.
[21] K. Wang, P.J. Teunissen, and A. El-Mowafy, “The ADOP and PDOP: Two complementary diagnostics for GNSS positioning,” *Journal of Surveying Engineering*, vol. 146, no. 2, p. 04020008, 2020.
[22] Tennessee Valley Authority, *Geospatial Positioning Accuracy Standards Part 3: National Standard for Spatial Data Accuracy*. Virginia, NV, USA: National Aeronautics and Space Administration, 1998.

Teetat Charoenkalunyuta holds a Ph.D. in Geomatics Engineering from Chulalongkorn University. He is an assistant professor in the Department of Survey Engineering, Faculty of Engineering, Chulalongkorn University, Bangkok, Thailand. His research focuses on GNSS surveying, CORS application, cadastral surveying and GIS application.

Chalermchon Satirapod holds a Ph.D. in GNSS Surveying from the University of New South Wales (UNSW), Australia. He is currently a full professor in the Department of Survey Engineering, Faculty of Engineering, Chulalongkorn University, Bangkok, Thailand. His research interests include new GNSS data processing techniques and quality-assured GNSS surveying for various static and kinematic applications.

Koltouch Anantakarn is pursuing a Master's degree in Survey Engineering at Chulalongkorn University, Thailand. He holds a B.Eng. in Civil Engineering from King Mongkut's Institute of Technology Ladkrabang, Thailand. His research interests focus on GNSS surveying.

Thayathip Thongtan holds a Ph.D. in Geomatics Engineering from University College London. She currently serves as an electrical metrologist at the Time and Frequency Laboratory, National Institute of Metrology, Thailand. Her research interests focus on GNSS applications for timing.